A buckling-based metrology for measuring the elastic moduli of polymeric thin films

CHRISTOPHER M. STAFFORD[1]*, CHRISTOPHER HARRISON[1†], KATHRYN L. BEERS[1], ALAMGIR KARIM[1], ERIC J. AMIS[1], MARK R. VANLANDINGHAM[2‡], HO-CHEOL KIM[3], WILLI VOLKSEN[3], ROBERT D. MILLER[3] AND EVA E. SIMONYI[4]

[1]Polymers Division, National Institute of Standards and Technology, Gaithersburg, Maryland 20899, USA
[2]Materials and Construction Research Division, National Institute of Standards and Technology, Gaithersburg, Maryland 20899, USA
[3]IBM Research Division, Almaden Research Center, San Jose, California 95120, USA
[4]IBM Research Division, T.J. Watson Research Center, Yorktown Heights, New York 10598, USA
[†]Present address: Sensor Physics Department, Schlumberger-Doll Research, Ridgefield, Connecticut 06877, USA
[‡]Present address: Polymers Research Branch, United States Army Research Laboratory, Aberdeen Proving Ground, Maryland 21005, USA
*e-mail: chris.stafford@nist.gov

Published online: 11 July 2004; doi:10.1038/nmat1175

As technology continues towards smaller, thinner and lighter devices, more stringent demands are placed on thin polymer films as diffusion barriers, dielectric coatings, electronic packaging and so on. Therefore, there is a growing need for testing platforms to rapidly determine the mechanical properties of thin polymer films and coatings. We introduce here an elegant, efficient measurement method that yields the elastic moduli of nanoscale polymer films in a rapid and quantitative manner without the need for expensive equipment or material-specific modelling. The technique exploits a buckling instability that occurs in bilayers consisting of a stiff, thin film coated onto a relatively soft, thick substrate. Using the spacing of these highly periodic wrinkles, we calculate the film's elastic modulus by applying well-established buckling mechanics. We successfully apply this new measurement platform to several systems displaying a wide range of thicknessess (nanometre to micrometre) and moduli (MPa to GPa).

Thin films are used increasingly in technological applications involving coatings, optical reflectors and filters, dielectric stacks and lithographic resists[1]. Although the mechanical properties and stability of these submicrometre-thick films are paramount for their effective utilization, there are currently few options for measuring such properties in thin-film systems[2]. Conventional mechanical testing devices typically do not have the sensitivity to measure the forces involved in straining a thin polymer film. Nanoindentation has proved successful in materials such as ceramics and some metals, but is challenged by soft materials, especially those of submicrometre thickness, or which exhibit significant viscoelastic behaviour[3]. Scanning probe microscopy has been used to measure the moduli of polymer films, but uncertainty in the tip size and/or contact area often limits the accuracy of these types of measurements, and researchers are challenged to obtain more than relative values[4,5]. In addition, available methodologies are not amenable or adaptable to high-throughput and/or combinatorial measurement techniques, which are proving to be critical for an increasingly fast-paced research environment.

In response, we introduce SIEBIMM (strain-induced elastic buckling instability for mechanical measurements), a technique that rapidly measures the elastic modulus of coatings and films[6]. The buckling phenomenon used by this technique is analogous to the observations by Bowden *et al.* in metal-coated or plasma-treated silicone sheets[7,8]. Several authors have derived the underlying mechanics governing the buckling of a supported film adhered to a soft elastic substrate[9–13]. We adapt these findings to deliver a versatile and quantitative measurement technique for determining the mechanical properties of thin films. As with any new measurement technique, we must validate the methodology on a series of model systems. To this end, we perform measurements on thickness gradients of polystyrene (PS) to establish the applicability of established buckling theory to interpret our data. Furthermore, because this method involves a rapid and intrinsically local measurement, we demonstrate that our technique is

©2004 Nature Publishing Group

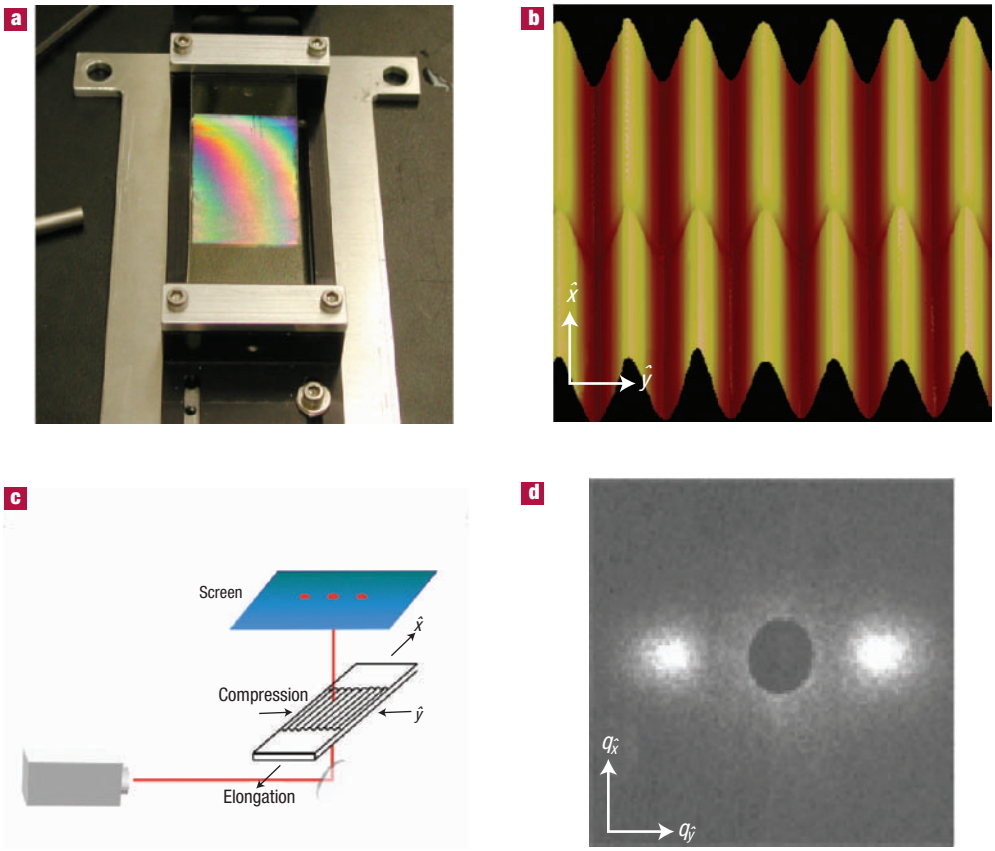

Figure 1 Experimental protocol and representative images illustrating the buckling instability of a thin polymeric film on a soft silicone sheet. a, A strained polymer film supported on a PDMS sheet clamped between two supports. The iridescent colour is a result of diffraction from micrometre-scale periodic ridges. **b**, Atomic force microscopy image of buckled film with amplitude 0.3 μm and wavelength 8 μm. **c**, Schematic of the custom-built small-angle light scattering apparatus. The diffraction pattern from the buckled film is projected onto a screen, and this pattern is acquired by CCD camera (not shown). **d**, Representative diffraction pattern centred on the beam-stop showing a positive and a negative order. The dominant wavenumber, q_0, is measured from the location of the diffraction peaks and the periodicity of the wrinkles, d, is given by $2\pi/q_0$.

well suited for quantitative screening of combinatorial libraries with spatially varying properties that can be prepared by existing methodologies developed at the National Institute of Standards and Technology (NIST) and elsewhere[14–18]. We also carry out measurements on plasticized polystyrene films to show the range of moduli that can be measured using this technique. Lastly, we apply this measurement methodology to a more complex and challenging system consisting of nanoporous organosilicate films being developed as low-k dielectrics for semiconductor applications.

Samples for SIEBIMM are prepared by transferring a thin film from a substrate (for example, silicon wafer, salt plate) to the surface of a relatively thick slab of polydimethylsiloxane (PDMS). The PDMS/film laminate is mounted onto a custom-built strain stage, and a buckling instability is induced by an applied compressional strain (Fig. 1a). The buckling instability is a result of the balance between the energy required to bend the stiff upper film and the energy required to deform the soft underlying substrate. There exists a critical wavelength that minimizes the total strain energy in the system, and this wavelength is dependent on the material properties of both the film and substrate[11–13]. Assuming a sinusoidal waveform of the buckling instability, the critical wavelength (d) can be expressed by

$$d = 2\pi h \left[\frac{(1-\nu_s^2)}{3(1-\nu_f^2)} \frac{E_f}{E_s} \right]^{1/3} \quad (1)$$

where h is the thickness of the upper film, ν is Poisson's ratio, and E is the Young's modulus (subscripts f and s denote the film and substrate, respectively). The atomic force micrograph in Fig. 1b confirms the sinusoidal deformation of the surface induced by the buckling instability. To clarify the typical length scales of the experiment, the micrograph shows a buckling wavelength for a PS film ($h \approx 100$ nm) of approximately 8 μm, yet the amplitude is only a few hundred nanometres for the applied strain in our experiments. Therefore, these buckles are better described as wrinkles on the surface of the PS/PDMS laminate. Equation (1) can be rearranged to solve for the modulus of the upper film:

$$\frac{E_f}{(1-\nu_f^2)} = \frac{3E_s}{(1-\nu_s^2)} \left(\frac{d}{2\pi h} \right)^3 \quad (2)$$

This solution assumes the plate is in a state of plane strain and requires that the Poisson's ratio of the film (ν_f) be known. The solution is valid in the limit of: (a) low strain ($\varepsilon << 10\%$), (b) $E_f/E_s >> 1$, (c) the substrate being much thicker than the film, and (d) the amplitude of the buckles is much smaller than their wavelength. In addition, these derivations assume elastic deformation of the materials, therefore yielding in the film negates the applicability of the measurement. (Another solution has been derived by Allen[10] for the case of an infinitely thin beam in the state of plane stress, which does not require the Poisson's ratio of the film to be known. Although Allen's model does not reflect the exact geometry

©2004 Nature Publishing Group

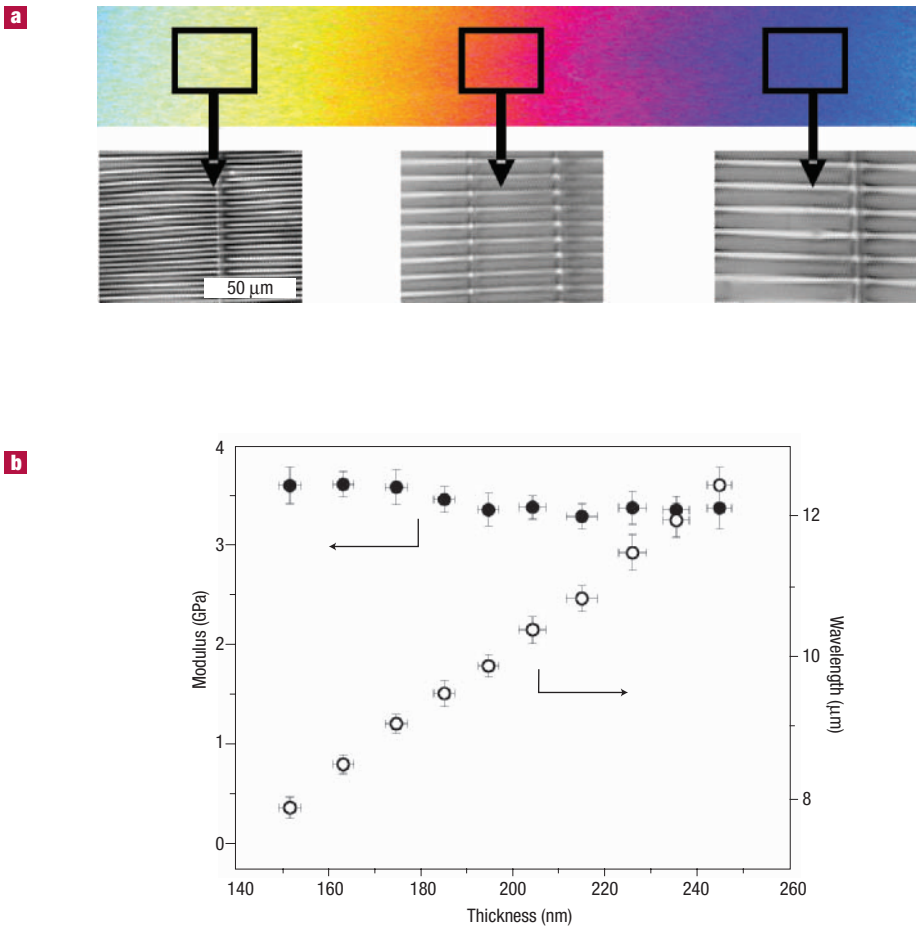

Figure 2 Modulus measurements of a thickness gradient film of PS. a, Optical micrograph of a PS thickness gradient on silicon wafer (140 nm to 280 nm). Greyscale insets show optical micrographs of the film after transfer to PDMS and application of strain to induce buckling. The doubling of the film thickness from left to right results in a doubling of the buckling period. **b**, Modulus versus thickness for a flow-coated thickness gradient sample. The linear increase in buckling wavelength (open circles) with film thickness confirms that the wrinkling instability is consistent with equation (2). The modulus (filled circles) remains largely constant (3.4 ± 0.1 GPa) over this thickness range, in good agreement with the reported bulk values. The error bars represent one standard deviation of the data, which is taken as the experimental uncertainty of the measurement.

of the systems studied here, it yields a reasonably accurate value for the modulus of the film without knowledge of the Poisson's ratio of the film. This may be advantageous when conducting high-throughput screening of material libraries in which the Poisson's ratio is unknown. For the systems studied here, applying Allen's model results in a calculated modulus of the upper film that is ≈10% lower than expected from equation (2).)

The dominant wavelength of the buckling instability can be measured by a variety of techniques including (but not limited to) laser diffraction, reflectance optical microscopy or atomic force microscopy. The choice of imaging technique depends on the relative length scale of the buckling wavelength in the system. For the systems discussed here, the wavelength of the buckling is determined by measuring the dominant wavenumber, q_0, obtained using small-angle light scattering of a low-power HeNe laser ($\lambda = 632.8$ nm) (see Fig. 1c), and using Bragg's Law as expressed by the following equation:

$$q_0 = \frac{4\pi}{\lambda}\sin\theta \approx \frac{2\pi}{d} \qquad (3)$$

where 2θ is the diffraction angle of the first order peak. A computer-controlled translation stage rasters the sample across the laser beam, thereby yielding spatially resolved diffraction patterns [$f(x,y)$], which are captured by a CCD (charge-coupled-device) camera. Spatially resolved sampling is advantageous to map out the mechanical properties of two-dimensional combinatorial libraries, as well as providing a convenient path for building statistically significant data sets on non-gradient sample specimens. Image acquisition time per point is less than one second and image analysis can be completed (using common software) in a few seconds, allowing hundreds of modulus measurements to be collected in a matter of minutes. Brittle samples, such as the polystyrene films examined here, may exhibit cracks running along the $\hat{y}$ axis, but we find that at low density these cracks do not interfere with our measurements.

We tested SIEBIMM with a film-thickness gradient of PS (atactic, $M_w = 2.80 \times 10^5$ g mol^{-1}, $M_w/M_n = 3.07$; M_w and M_n are weight- and number-average molecular weight respectively) ranging from 150 nm to 240 nm (Fig. 2a). The film thickness was mapped ($h(x,y)$) with a reflectance interferometer, confirming a monotonic increase in thickness along the long axis ($\hat{x}$) and uniformity along the orthogonal

©2004 Nature Publishing Group

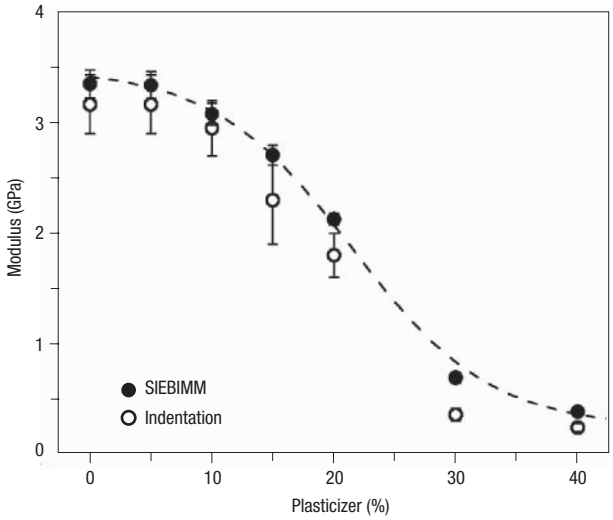

Figure 3 Modulus versus plasticizer concentration (dioctyl phthalate) for thin PS films. SIEBIMM measurements (filled circles) and nanoindentation measurements (open circles) showing the modulus decreases monotonically with increasing concentration of plasticizer in the film. The thickness (h) of the films ranged from 110 nm to 130 nm. The data are fit to a sigmoidal function (dashed line) as a guide to the eye. The error bars represent one standard deviation of the data, which is taken as the experimental uncertainty of the measurement. Some error bars are smaller than the symbols.

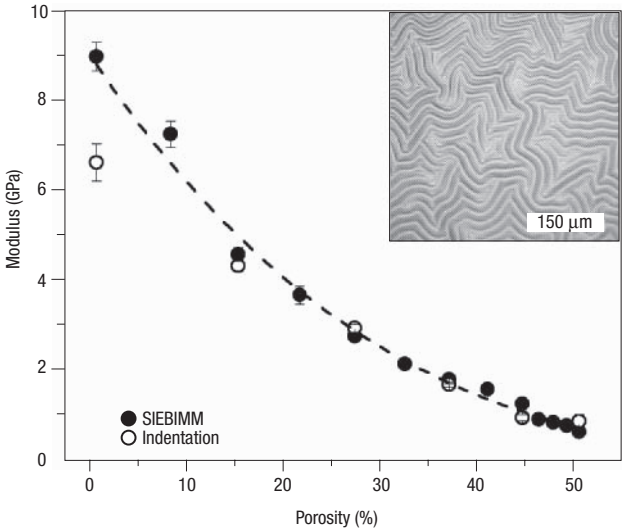

Figure 4 Modulus versus porosity for a series of nanoporous organosilicate films. SIEBIMM measurements (filled circles) and nanoindentation measurements (open circles) show excellent agreement through the entire range of porosity. The modulus dramatically decreases from 9 GPa to 0.6 GPa as the porosity increases. The curve fit of the SIEBIMM data to the Phani and Nyogi model[29] is represented by a dashed line. The error bars represent one standard deviation of the data, which is taken as the experimental uncertainty of the measurement. Some error bars are smaller than the symbols. Inset: Optical image of the isotropic buckling of a PDMS-supported nanoporous film.

axis ($\hat{y}$). Although we have incorporated sample variation (thickness) along only one direction, a second parameter could be varied in an orthogonal direction to make a two-dimensional gradient sample, well-suited to combinatorial investigations. The sample was transferred to PDMS, the PS/PDMS was strained to induce buckling and the dominant wavelength ascertained by small-angle light scattering. The buckling wavelength, d, increases linearly with film thickness (Fig. 2b, right axis), consistent with equation (2). The film modulus, E_f, is calculated from equation (2), using a Poisson's ratio of the PS film of $\nu_f = 0.33$ (ref. 19). In our experiments, E_s varied in the range (1.5–2.0) ± 0.1 MPa depending on the exact mixing ratio, curing profile, and batch-to-batch variability of the PDMS. The measured values of E_f (Fig. 2b, left axis) for atactic PS show that the modulus is constant (within error bars) over this thickness range. In fact, we have conducted SIEBIMM measurements on films as thin as 30 nm and the measured modulus remains 3.4 ± 0.1 GPa. This thickness regime ($h \approx R_g$) is currently inaccessible by nanoindentation for studying polymer thin films and promises to be a rich and exciting area for further study. The limitation in measuring the modulus of thinner films ($h < 30$ nm) lies not in the technique, but rather in the inability of interferometry to measure films of this thickness accurately, which is crucial to obtaining accurate values for modulus. More sensitive thickness measurements (for example, X-ray reflectivity) will enable accurate modulus measurements of polymer films with nanometre-scale thickness, which will be described in a subsequent publication. SIEBIMM measurements are in agreement with three-point bend measurements on bulk samples of the same material, and are consistent with typical values reported in the literature[19].

Another model system consisted of mixtures of PS and a non-volatile plasticizer, dioctyl phthalate, co-dissolved in toluene, which were spin-cast onto silicon wafers. SIEBIMM data in Fig. 3 (filled circles) show that the modulus decreases in a sigmoidal manner as the plasticizer concentration increases. The shape of the curve is strikingly similar to conventional plasticizer curves for bulk samples of plasticized poly(vinyl chloride)[20]. Nanoindentation was performed on PS films equivalent to those measured by SIEBIMM. Films with thicknesses ranging from approximately 200 nm to 500 nm cast on silicon wafers were indented using a NanoIndenter DCM (MTS Systems; see Methods) with a Berkovich pyramidal tip[21]. Nanoindentation and SIEBIMM data show good agreement, within the error of the experiment, for plasticizer levels below 20%, but discrepancies appear for samples with higher plasticizer weight fractions (Fig. 3, open circles). The discrepancy in the SIEBIMM measurement may arise from diffusion of plasticizer from the polymer film into the PDMS substrate that could change the plasticizer concentration in the polymer, resulting in a higher modulus to be measured than anticipated. In addition, the low-frequency experimental observations of buckling in such highly plasticized films shown here should stimulate further discussion and encourage the development of analytical solutions to address the transition from elastic-on-elastic systems to viscoelastic-on-elastic systems. We note this wrinkling instability has been routinely demonstrated on materials with moduli down to 5 MPa, suggesting that SIEBIMM is applicable to such soft materials with the proper analysis.

In addition to these model systems, we also applied SIEBIMM to measure the mechanical properties of nanoporous low-k dielectrics in development for semiconductor applications. The modulus of these low-k films has been well correlated with their resilience to the chemical–mechanical polishing used during processing. Although the exact requirements for the modulus of low-k materials has yet to be established, literature reports have advocated that interlayer dielectrics should have a modulus greater than 4 GPa in order to display resilience to chemical–mechanical polishing and planarization processes[22].

©2004 Nature Publishing Group

Measurement of these properties has been challenging and time-consuming using conventional methodologies. In contrast, SIEBIMM is effective and simple for measuring the properties of nanoporous films consisting here of a matrix of methylsilsesquioxane–silica copolymer mixture and a thermally labile pore generator[23].

For SIEBIMM measurement, thin films were spin-coated onto salt plates from a solution of methylsilsesquioxane and porogen and annealed to volatilize the labile component[24]. A parallel set of identical samples was spin-coated onto silicon wafers for film thickness measurements by ellipsometry. Porogen loadings varied from 0 to 0.50 mass fraction with resulting porosities ranging from 0 to 0.51 percent as determined by X-ray reflectivity[25]. Films were chemically bonded to PDMS sheets with ultraviolet (UV)/ozone exposure[26,27] and the salt substrate was subsequently dissolved away. Residual stress in the films was sufficient to spontaneously wrinkle the PDMS sheet. Because the stresses generated during thermal processing are isotropic, the resulting buckling patterns (Fig. 4, inset) are no longer oriented in one direction as in the case of the model systems. Optical microscopy was used to characterize the buckling in these specimens because the typical buckling wavelength ($h \approx 725$ nm) was of the order of 30 μm. The buckling wavelength was ascertained by a Fourier transform of the optical image, and we calculated the modulus of the nanoporous films and present the SIEBIMM results in Fig. 4 (filled circles). The Poisson's ratio for these materials has been reported[28] to be $\nu_f = 0.26$, and this value was used in equation (2). These measurements show that the modulus decreases rapidly with increasing porosity, in good agreement with nanoindentation (Fig. 4, open circles) on identical films supported on silicon. A critical feature of the buckling instability is that the amplitude of the buckles varies as a function of the applied strain[12,13]. For the nanoporous films, the applied strain is equivalent to the residual strain in the films (that is, spontaneous buckling with no applied strain); therefore, one could obtain an estimate of the residual stress in these types of films simply by measuring the amplitude of the buckling pattern. This aspect will be explored in more detail in a future publication.

We evaluated several models of effective elastic moduli that describe the porosity dependence of modulus; we find that the semi-analytical approach of Phani and Niyogi best describes our data while providing insight into material structure[29]. Accordingly, we fit our moduli data to the following equation (Fig. 4, dashed line):

$$E_f = E_0(1 - aP)^n \quad (4)$$

where E_0 is the modulus of the matrix and P is the porosity, and a and n are material constants. From this fit, we ascertain a and n to be 1 and 3.45, respectively. These values are similar to those measured for other porous materials with irregularly shaped pores, such as alumina[30]. This is reasonable because the nature of the phase-separation mechanism used to generate pores in these materials provides isotropic porous structures with random morphology[31,32]. Furthermore, our measurements are generally in good agreement with finite-element computations for similar structures at low porosity, although to our knowledge, calculations have yet to be performed for the exact morphology of our materials[33]. The good agreement between SIEBIMM and nanoindentation moduli suggests that SIEBIMM can provide an inexpensive, fast, and highly effective technique for researchers developing these new low-k dielectric materials. Moreover, our technique is positioned to measure accurately the moduli of nanoporous films in a thickness regime ($50 \text{ nm} < h < 250 \text{ nm}$) where similar measurements by nanoindentation are highly convoluted by substrate effects. We expect that this technique will find application in addressing a variety of questions ranging from fundamental materials science to applied discovery in the field of films and coatings.

METHODS

GENERAL

Equipment and instruments or materials are identified in the paper in order to adequately specify the experimental details. Such identification does not imply recommendation by NIST, nor does it imply the materials are necessarily the best available for the purpose.

SAMPLE PREPARATION

Silicon wafers for film preparation were cleaned with a UV source (Model 342, Jelight) for 20 minutes to make the surface hydrophilic. Polymer films of uniform thickness were spin-cast from dilute polymer solutions, and films with thickness gradients were prepared by flow-coating dilute polymer solutions using an accelerating knife blade[34]. The thickness of the films on silicon was measured with a UV–visible interferometer (Model F20, Filmetrics) operated in reflectance mode. PDMS was prepared as suggested by the manufacturer (Sylgard 184, Dow Corning) at a ratio of 10:1 (by mass) of base to curing agent. The modulus of the PDMS was measured before each experiment using a Texture Analyzer (Model TA.XT2i, Texture Technologies). A PDMS sheet (typical dimensions 25 mm × 75 mm × 2 mm) was placed onto the supported polymer film, which was then immersed in water. Water wets the interface between the hydrophilic wafer and the polymer film, thereby transferring the film from the wafer onto the PDMS. Measurements were taken after samples were dried under vacuum for several hours.

AFM images were acquired on a Dimension 3100 (Veeco Instruments). Optical images were acquired on a Nikon Optiphot microscope equipped with a Kodak ES 1.0 CCD camera.

INDENTATION OF PLASTICIZED POLYSTYRENE FILMS

Indentation of plasticized films was performed on a NanoIndenter DCM (MTS Systems). A small dynamic oscillation with frequency and harmonic amplitude controlled at 75 Hz and 5 nm was superimposed over the loading segment, which was controlled to have a constant ratio of load rate to load of 0.05 s^{-1} (note that frequencies of 10 Hz and 250 Hz and a load rate to load ratio of 0.01 s^{-1} were also used in the testing of several samples). The indentation modulus was calculated directly from the in-phase dynamic response using a dynamic model of the system. Indentation data was insensitive to the tip-oscillation frequency and loading rate.

SURFACE TREATMENT OF NANOPOROUS LOW-K FILMS

We find that for thick organosilicate films ($h \approx 725$ nm), a mild surface treatment of the films is necessary to enhance the adhesion between the nanoporous films and the PDMS substrates. UV/ozone treatment was chosen as the method of surface treatment owing to the mild nature of UV/ozone in comparison with oxygen plasma, while still producing surface silanols groups that can chemically bond at the interface of the film and PDMS. Treatment of organosilicates with UV/ozone will change the surface properties of the film and, if the pores are interconnected, could also alter the properties of the interior of the film. The data presented here were collected on samples that were treated with 60 min of UV/ozone, but subsequent experiments indicated that 0.5 min of UV/ozone was sufficient to adhere the organosilicate to the PDMS substrate with no apparent change in the modulus within the error of the experiment. The surface of the PDMS was also exposed to UV/ozone for 0.5 min, which does not lead to significant changes in the surface modulus of the PDMS (ref. 27).

INDENTATION OF NANOPOROUS LOW-K FILMS

Indention was performed on a NanoIndenter XP (MTS Systems) with a small oscillatory force superimposed over the loading segment. A minimum of 20 indentation experiments were carried out for each sample.

Received 1 April 2004; accepted 3 June 2004; published 11 July 2004.

References

1. Elshabini-Riad, A. A. R. & Barlow, F. D. *Thin Film Technology Handbook* (McGraw-Hill, New York, 1997).
2. Asif, S. A. S., Wahl, K. J. & Colton, R. J. Nanoindentation and contact stiffness measurement using force modulation with a capacitive load-displacement transducer. *Rev. Sci. Instrum.* **70,** 2408–2413 (1999).
3. VanLandingham, M. R., Villarrubia, J. S., Guthrie, W. F. & Meyers, G. F. Nanoindentation of polymers: An overview. *Macromol. Symp.* **167,** 15–43 (2001).
4. Du, B. Y. *et al.* Nanostructure and mechanical measurement of highly oriented lamellae of melt-drawn HDPE by scanning probe microscopy. *Macromolecules* **33,** 7521–7528 (2000).
5. Du, B. Y., Tsui, O. K. C., Zhang, Q. L. & He, T. B. Study of elastic modulus and yield strength of polymer thin films using atomic force microscopy. *Langmuir* **17,** 3286–3291 (2001).
6. Stafford, C. M., Harrison, C., Karim, A. & Amis, E. J. Measuring the modulus of polymer films by strain-induced buckling instabilities. *Polymer Preprints* **43,** 1335 (2002).
7. Bowden, N., Brittain, S., Evans, A. G., Hutchinson, J. W. & Whitesides, G. M. Spontaneous formation of ordered structures in thin films of metals supported on an elastomeric polymer. *Nature* **393,** 146–149 (1998).
8. Bowden, N., Huck, W. T. S., Paul, K. E. & Whitesides, G. M. The controlled formation of ordered, sinusoidal structures by plasma oxidation of an elastomeric polymer. *Appl. Phys. Lett.* **75,** 2557–2559 (1999).
9. Biot, M. A. Bending of an infinite beam on an elastic foundation. *J. Appl. Mech. A* **4,** 1–7 (1937).
10. Allen, H. G. *Analysis and Design of Structural Sandwich Panels* (Pergamon, New York, 1969).
11. Volynskii, A. L., Bazhenov, S., Lebedeva, O. V. & Bakeev, N. F. Mechanical buckling instability of thin coatings deposited on soft polymer substrates. *J. Mater. Sci.* **35,** 547–554 (2000).
12. Groenewold, J. Wrinkling of plates coupled with soft elastic media. *Physica A* **298,** 32–45 (2001).
13. Huang, R. in *UT-MSSM Report No. 04/01* 1–48 (Univ. Texas, Austin, 2004).
14. Meredith, J. C., Karim, A. & Amis, E. J. Combinatorial methods for investigations in polymer materials science. *Mater. Res. Soc. Bull.* **27,** 330–335 (2002).
15. Lenhart, J. L. *et al.* Combinatorial methodologies offer potential for rapid research of photoresist materials and formulations. *J. Vac. Sci. Technol. B* **20,** 704–709 (2002).
16. Meier, M. A. R., Hoogenboom, R. & Schubert, U. S. Combinatorial methods, automated synthesis and high-throughput screening in polymer research: The evolution continues. *Macromol. Rapid Comm.* **25,** 21–33 (2004).

©2004 Nature Publishing Group

17. Schmatloch, S., Bach, H., van Benthem, R. & Schubert, U. S. High-throughput experimentation in organic coating and thin film research: State-of-the-art and future perspectives. *Macromol. Rapid Comm.* **25,** 95–107 (2004).
18. Cawse, J. N. Experimental strategies for combinatorial and high-throughput materials development. *Acc. Chem. Res.* **34,** 213–221 (2001).
19. Brandrup, J., Immergut, E. H. & Grulke, E. A. (eds) *Polymer Handbook* (Wiley, New York, 1999).
20. Sears, J. K. & Darby, J. R. *The Technology of Plasticizers* (Wiley, New York, 1982).
21. VanLandingham, M. R. Review of instrumented indentation. *J. Res. Natl Inst. Stan.* **108,** 249–265 (2003).
22. Wetzel, J. T. *et al.* Evaluation of material property requirements and performance of ultra-low dielectric constant insulators for inlaid copper metallization. *IEDM Tech. Digest* 73–75 (2001).
23. Miller, R. D. Device physics - In search of low-k dielectrics. *Science* **286,** 421–423 (1999).
24. Volksen, W. *et al.* in *Low Dielectric Constant Materials for IC Applications* (eds Ho, P. S., Leu, J. & Lee, W. W.) 167–202 (Springer, New York, 2003).
25. Grill, A. *et al.* Porosity in plasma enhanced chemical vapor deposited SiCOH dielectrics: A comparative study. *J. Appl. Phys.* **94,** 3427–3435 (2003).
26. Duffy, D. C., McDonald, J. C., Schueller, O. J. A. & Whitesides, G. M. Rapid prototyping of microfluidic systems in poly(dimethylsiloxane). *Anal. Chem.* **70,** 4974–4984 (1998).
27. Efimenko, K., Wallace, W. E. & Genzer, J. Surface modification of Sylgard-184 poly(dimethyl siloxane) networks by ultraviolet and ultraviolet/ozone treatment. *J. Colloid Interface Sci.* **254,** 306–315 (2002).
28. Flannery, C. M., Wittkowski, T., Jung, K., Hillebrands, B. & Baklanov, M. R. Critical properties of nanoporous low dielectric constant films revealed by Brillouin light scattering and surface acoustic wave spectroscopy. *Appl. Phys. Lett.* **80,** 4594–4596 (2002).
29. Phani, K. K. & Niyogi, S. K. Young modulus of porous brittle solids. *J. Mater. Sci.* **22,** 257–263 (1987).
30. Knudsen, F. P. Effect of porosity on Young's modulus of alumina. *J. Am. Ceram. Soc.* **45,** 94–95 (1962).
31. Huang, E. *et al.* Pore size distributions in nanoporous methyl silsesquioxane films as determined by small angle x-ray scattering. *Appl. Phys. Lett.* **81,** 2232–2234 (2002).
32. Hedstrom, J. A. *et al.* Pore morphologies in disordered nanoporous thin films. *Langmuir* **20,** 1535–1538 (2004).
33. Roberts, A. P. & Garboczi, E. J. Elastic properties of model porous ceramics. *J. Am. Ceram. Soc.* **83,** 3041–3048 (2000).
34. Meredith, J. C., Smith, A. P., Karim, A. & Amis, E. J. Combinatorial materials science for polymer thin-film dewetting. *Macromolecules* **33,** 9747–9756 (2000).

Acknowledgements

We acknowledge insightful discussions with Rui Huang, Michael J. Fasolka, Jack F. Douglas, Richard A. Register, Edward J. Garboczi and Jan Groenewold. We thank Donald Hunston and Sheng Lin-Gibson for measurement assistance. C.M.S. and C.H. acknowledge the NIST National Research Council Postdoctoral Fellowship Program and funding from the MSEL Director's Reserve Program.
Correspondence and requests for materials should be addressed to C.M.S.

Competing financial interests

The authors declare that they have no competing financial interests.

©2004 Nature Publishing Group